# MODELLING CHEMICAL-LOOPING ASSISTED BY OXYGEN UNCOUPLING (CLaOU): ASSESSMENT OF NATURAL GAS COMBUSTION WITH CALCIUM MANGANITE AS OXYGEN CARRIER

**Alberto Abad[*], Pilar Gayán, Luis F. de Diego, Francisco García-Labiano, Juan Adánez**

**Instituto de Carboquímica (ICB-CSIC), Miguel Luesma Castán 4, 50018, Zaragoza, Spain**

**[*] Corresponding author:**
**e-mail: abad@icb.csic.es**

## Supplementary Material

### 1. The Chemical Looping Combustion unit

A fuel reactor model was validated against experimental results obtained in the CLC unit at Vienna University of Technology (TUV). For this purpose, theoretical predictions were compared to experimental results obtained under 29 different operational conditions.

Dimensions and operational conditions for the Dual Circulating Fluidised Bed Concept (DCFB) unit at TUV are considered for both the fuel and air reactor (Pröll et al., 2009). Fig. A1 shows a scheme of this unit. The CLC system combines two circulating fluidised bed reactors with direct hydraulic communication via a loop seal. Very high solids circulation flow rate is reached with this CLC concept. Table A1 shows the main dimensions of the fuel reactor. The fuel reactor has an internal circulation of solids via a cyclone and the internal loop seal. Steam is used to fluidize the internal loop seal, which goes mostly to the fuel reactor. The bottom of the fuel reactor is fluidized by the fuel gas, while steam fluidizing the lower loop seal mostly enters to the air reactor.

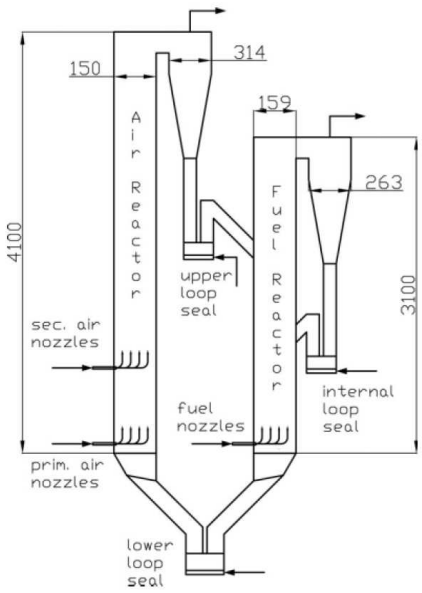


Fig. A1. Schematic diagram of the DCFB unit.

Table A1. Geometrical parameters of the fuel and air reactors in the DCFB unit.

| | Fuel reactor |
|---|---|
| Height, $H_r$ (m) | 3.0 |
| Diameter, $d_{react}$ (m) | 0.159 |
| Height for inlet gas from loop seals [(1)] (m) | 0.35 |
| Height for inlet solids from loop seals [(2)] (m) | 2.0 |

[(1)] Steam from internal loop seal.

[(2)] Solids and steam from upper loop seal.

The fluid dynamics of the fuel reactor was adapted to the characteristics of the CLC unit, which is a Dual Circulating Fluidised Bed (DCFB) system. In addition, the recirculated oxygen carrier enters to the fuel reactor 2 m above the fuel inlet, where the transport phase is dominating. This fact has implications on solids concentration profile and fuel conversion in the transport phase, which are considered in the model.

## 2. Fluid dynamic model

The fuel reactor is considered to be a fluidised bed working at the turbulent regime. The fluid dynamic model considers the gas and solids flows inside the reactor and the gas-solids mixing patterns in the different reactor regions in which it can be divided. The fluid dynamic model was described in Abad et al. (2013). A brief description of the fluid dynamical model is now presented.

The model considers the reactor divided into two vertical zones with respect to axial concentration and backmixing of solids, see Fig. A2: 1) a bottom or dense bed with a high and roughly constant solids concentration; and 2) a freeboard or dilute region above the dense bed, where there is a pronounced decay in solids concentration with height.

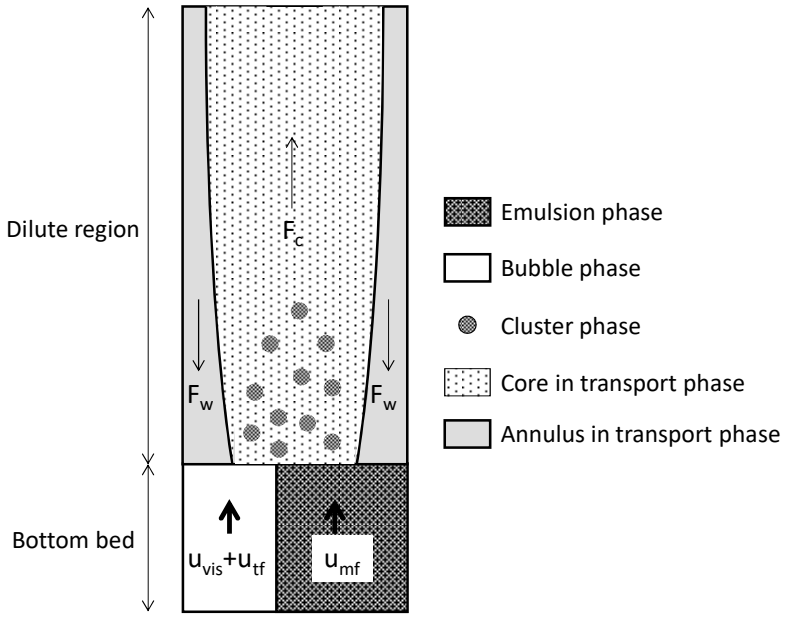


Fig. A2. Gas and solids distribution in the high-velocity fluidised bed reactors.

Different behaviour for the solids is assumed for the cluster and the transport phases, which affects to the reactivity of the particles in every phase. Solids into the cluster phase are in perfect mixing with the dense bed. These particles have the same average solids conversion in all positions inside the reactor. On the contrary, solids in the transport phase have a net flow up through the core. Thus, the solids conversion increases as the solids flow up through the core.

Special attention was paid on the inlet stream of solids to the fuel reactor coming from the air reactor through the upper loop seal. This stream of solids is added to the transport phase and modifies the solids distribution in the dilute region of the fuel reactor, thus modifying the fuel conversion in this zone. First, the solids concentration is increased, as it was considered in the description of the fluid dynamic behaviour of the reactor. Second, this stream of solids has a different conversion than solids in the fuel reactor because these particles are just oxidised in the air reactor.

2.1. Fluid dynamic in the dense bed

Gas distribution and mixing between the emulsion and bubble in the dense bed is considered. Thus, the gas flow in the dense bed is shared between the emulsion and bubble phases, with gas mixing between them controlled by diffusion. Solids are in the emulsion phase, where gas flow maintains the minimum fluidizing conditions, $u_{mf}$; whereas the rest of gas goes through visible bubbles, $u_{vis}$, and throughflow, $u_{tf}$, where there are not solids. Thus, in terms of superficial gas velocities the total gas flow, $u_g$, is divided following the equation

$$u_g = (1-\delta_b)u_{mf} + u_{vis} + u_{tf} \quad \text{(A1)}$$

Thus, the gas flow through the emulsion depends on the fraction of volume occupied by emulsion, i.e. (1- $\delta_b$), and $u_{mf}$. The minimum fluidization velocity, $u_{mf}$, is calculated using the following correlation (Grace, 1986):

$$\mathrm{Re}_{\mathrm{p,mf}} = \frac{u_{mf}\rho_g d_p}{\mu_g} = \sqrt{27.2^2 + 0.0408\mathrm{Ar}} - 27.2 \quad \text{(A2)}$$

The bubble fraction, $\delta_b$, depends on the expansion of the bed compared to minimum fluidization conditions, i.e. the porosity of emulsion, $\varepsilon_{mf}$, and the actual porosity of the bed, $\varepsilon_b$:

$$\delta_b = \frac{\varepsilon_b - \varepsilon_{mf}}{1 - \varepsilon_{mf}} \quad \text{(A3)}$$

The porosity at minimum fluidization conditions is calculated with the following equation (Broadhurst and Becker, 1975):

$$\varepsilon_{mf} = 0.586\phi_{sh}^{-0.72}\mathrm{Ar}^{-0.029}\left(\frac{\rho_g}{\rho_s}\right)^{0.021} \quad \text{(A4)}$$

whereas the bed porosity depends on the gas velocity of rising bubbles, $u_{vis}$.

$$\varepsilon_b = \varepsilon_{mf} - \frac{u_{vis}}{u_{vis} - 0.71\sqrt{g d_b}}\left(1-\varepsilon_{mf}\right) \tag{A5}$$

$d_b$ being the bubble size, which is calculated with the equation proposed by Darton et al. (1977).

$$d_b = 0.54\left(u_g - u_{mf}\right)^{0.4}\left(z + 4\sqrt{A_0}\right)^{0.8} g^{-0.2} \tag{A6}$$

The solids concentration can be calculated as:

$$C_{db} = \rho_s\left(1-\varepsilon_b\right) \tag{A7}$$

The bed porosity increases with the gas velocity up to the saturation value is reached, $\varepsilon_{b,sat}$:

$$\varepsilon_{\mathrm{b,sat}} = 0.5452 + \frac{495.5}{\Delta P_0} + \frac{4.9\cdot 10^{-6}}{d_p} \tag{A8}$$

A higher value in the bed porosity than $\varepsilon_{b,sat}$ is not allowed, and the excess of gas goes directly to the throughflow, $u_{th}$. So, the excess of gas in bubbles is shared between gas in visible bubbles and throughflow defined by the ratio of the visible bubble flow to the total flow through the bubbles,$\Psi$, calculated as

$$\psi = \frac{0.26 + 0.70e^{-3300 d_p}}{\left(0.15 + u_g - u_{mf}\right)^{1/3}}\left(z + 4\sqrt{A_0}\right)^{0.4} \tag{A9}$$

Thus, the visible bubble flow is calculated as follows:

$$u_{vis} = \psi\left(u_g - u_{mf}\left(1-\delta_b\right)\right) \tag{A10}$$

excepting for the saturation conditions, i.e. when $\varepsilon_{b,sat} < \varepsilon_b$ (by eq. 5), where $u_{vis}$ is calculated by

$$u_{vis} = u_{vis,sat} = \frac{\delta_{\mathrm{b,sat}}}{1-\delta_{\mathrm{b,sat}}} u_{b\infty} \tag{A11}$$

Once $u_{mf}$, $\delta_b$ and $u_{vis}$ are known, $u_{tf}$ is calculated with equation (A1).

2.2. Fluid dynamic in the dilute region

The dilute region is composed by the cluster phase and a transport or dispersed phase. Both the cluster and transport phases are superimposed but with different mixing behaviour. The cluster phase has a strong solids backmixing with solids in the dense bed, and the solids concentration in this phase is given by the decay factor *a*:

$$\frac{\mathrm{d}C_{cl}}{\mathrm{d}z} = -aC_{cl} \tag{A12}$$

$$a = 4\frac{u_t}{u_g} \tag{A13}$$

The transport phase is characterized by a core/annulus flow structure. A net flow up of solids goes through the core and particles backmixing occurs at annulus near the reactor walls. Solids at the annulus go until the dense bed. The gas flows up through the core, which diameter just above the dense bed is calculated with the following equation:

$$D_C = 0.87D_r \tag{A14}$$

The diameter of the core section is maintained constant up to the saturation height, $z_{sat}$:

$$z_{sat} = H_r - 6D_r \tag{A15}$$

Then, the diameter of the core increases from the saturation height up to reach the exit zone of solids to cyclone.

$$D_C = D_r - 0.0217\left(H_r - z\right) \tag{A16}$$

The solids concentration in the core section decreases with the reactor height, and it is calculated with the following equations:

$$\frac{\mathrm{d}C_{tr}}{\mathrm{d}z} = -KC_{tr} \tag{A17}$$

$$K = \frac{0.23}{u_g - u_t} \tag{A18}$$

A direct relation between solids flow and solids concentration in the transport phase is given by the following equation, which considers the variation of both the gas velocity and core section with height:

$$F_{tr} = C_{tr}A_C\left(u_g - u_t\right) \tag{A19}$$

The boundary condition for differential equations (A12) and (A17) are given by equations (A20) and (A21), which consider the flow of solids entrained from the dense bed to the transport phase (de Diego et al., 1995) and a continuity balance of solids between the dense bed and the dilute region. Moreover, the gas and solids flows coming from the upper loop seal of the DCFB unit, $Q_{g,ULS}$ and $F_s$, are added to the gas stream in the core and the transport phase, respectively.

$$F_{tr,H_b} = 131.1\left[\frac{A_C u_g}{\varepsilon_b}\rho_g\left(\frac{\mathrm{Re}_s}{\mathrm{Ar}}\right)^{0.31}\right]_{H_b} \tag{A20}$$

$$C_{cl,H_b} = C_{db,H_b} - C_{tr,H_b} \tag{A21}$$

$$u_{g,H_{ULS}^{+}} = u_{g,H_{ULS}^{-}} + \frac{Q_{g,ULS}}{A_C} \tag{A22}$$

$$F_{tr,H_{ULS}^{+}} = F_{tr,H_{ULS}^{-}} + F_s \tag{A23}$$

Once the solids flow in the core section is known, the net lateral flow of solids from the core to annulus next the reactor wall can be calculated:

$$\frac{\mathrm{d}F_w}{\mathrm{d}z} = -\frac{\mathrm{d}F_{tr}}{\mathrm{d}z} \tag{A24}$$

The boundary condition for equation (A23) is given at the position of the exit to cyclone. From the solid flow upward at the height of the output, a fraction reach the cyclone, $F_s$, and another fraction goes downward by the annulus, $F_{w,H_r}$. The backflow ratio, $k_b$, relates both flows of solids, and depends on the entrainment probability of a particle in the exit zone (Pallarès and Johnsson, 2006):

$$k_b = \frac{F_{w,H_r}}{F_s} = \frac{1}{p_{ent}} - 1 \tag{A25}$$

$$p_{ent} = \frac{1}{\left(4.07 - u_{slip}\right)^{0.5}} \qquad \text{for } u_{slip} < 3.07 \text{ m/s} \tag{A26}$$

$$p_{ent} = 1 \qquad \text{for } u_{slip} > 3.07 \text{ m/s} \tag{A27}$$

**3. Mass balances into the reactors**

Mass balances for the different reacting compounds and products are developed for each phase in the dense bed and the dilute region. The pathway for methane conversion in the fuel reactor with the oxygen carrier is described by the following reaction:

$$3\ M_xO_y\ (s)\ +\ CH_4\ (g)\ \rightarrow\ 3\ M_xO_{y-1}\ (s)\ +\ CO\ (g)\ +\ 2\ H_2O\ (g) \qquad (A28)$$

$H_2O$ is considered a primary product of the methane combustion and CO is considered as an intermediate product, which can react with steam in gases following the forward water-gas shift (fWGS) reaction or with the oxygen carrier to form $CO_2$ (Dewaele and Froment, 1999). Subsequently, $H_2$ produced in the WGS reaction can react with the oxygen carrier.

$$CO\ (g)\ +\ H_2O\ (g)\ \rightarrow\ CO_2\ (g)\ +\ 2\ H_2\ (g) \qquad (A29)$$

$$M_xO_y\ (s)\ +\ CO\ (g)\ \rightarrow\ M_xO_{y-1}\ (s)\ +\ CO_2\ (g) \qquad (A30)$$

$$M_xO_y\ (s)\ +\ H_2\ (g)\ \rightarrow\ M_xO_{y-1}\ (s)\ +\ 2\ H_2O\ (g) \qquad (A31)$$

In this model the oxygen uncoupling reaction of the oxygen carrier is also considered. Then, gaseous oxygen is evolved from the solid oxygen carrier, which can react with gaseous fuels ($CH_4$, CO or $H_2$) in a homogeneous reaction.

$$2\ M_xO_y\ (s)\ \rightarrow\ 2\ M_xO_{y-1}\ (s)\ +\ O_2\ (g) \qquad (A32)$$

$$CH_4\ (g)\ +\ 1.5\ O_2\ (g)\ \rightarrow\ CO\ (g)\ +\ 2\ H_2O\ (g) \qquad (A33)$$

$$CO\ (g)\ +\ 0.5\ O_2\ (g)\ \rightarrow\ CO_2\ (g) \qquad (A34)$$

$$H_2\ (g)\ +\ 0.5\ O_2\ (g)\ \rightarrow\ H_2O\ (g) \qquad (A35)$$

Mass balances are considered in the model for every compound in each phase described in the fluid dynamic model. Mass balances are given by the following differential equations for each gas, i.e. $CH_4$, CO, $H_2$, $CO_2$, $H_2O$ and $O_2$ in the fuel reactor:

Emulsion:

$$\frac{dF_{e,i}}{dV} = \frac{d\left[\left(1-\delta_b\right)u_{mf}C_{e,i}\right]}{dz} = -\left(1-\delta_b\right)\sum_k\left(-\overline{r}_{g,i}\right)_{e,k} - \delta_b k_{be}\left(C_{e,i}-C_{b,i}\right) - y_{e,i}\frac{dF_{exc}}{dV} \qquad (A36)$$

Bubble:

$$\frac{dF_{b,i}}{dV} = \frac{d\left[\left(u_{vis}+u_{tf}\right)C_{b,i}\right]}{dz} = -\delta_b\sum_k\left(-\overline{r}_{g,i}\right)_{b,k} + \delta_b k_{be}\left(C_{e,i}-C_{b,i}\right) + y_{e,i}\frac{dF_{exc}}{dV} \qquad (A37)$$

Dilute region:

$$\frac{dF_{dil,i}}{dV} = \frac{d\left[u_g C_{dil,i}\right]}{dz} = -\xi_{g-s}\left[\sum_k \left(-\overline{r}_{g,i}\right)_{cl,k} + \sum_k \left(-\overline{r}_{g,i}\right)_{tr,k}\right] \quad \text{(A38)}$$

Mass balances include the main processes by which a compound can appear or disappear in a phase. The following processes are considered:

a) $\left(-\overline{r}_{g,i}\right)_{j,k}$ is the average reaction rate of the gas *i* by reaction *k* with the gas concentration in the phase *j*. Heterogeneous reactions happen only in the emulsion phase and dilute region, i.e. where solids are present. In the bubble phase uniquely homogeneous reactions are considered.

b) Diffusional gas exchange between bubbles ($u_{vis}$ and $u_{tf}$) and emulsion ($u_{mf}$) in the dense phase, which is determined by the bubble-emulsion gas exchange coefficient, $k_{be}$. In the dilute region, the gas mixing behaviour is considered by the use of a contact efficiency parameter between gas and solids, $\xi_{g\text{-}s}$ (Furusaki et al., 1976).

$$\xi_{g-s}(z) = 1 - 0.75\left(\frac{C_{dil}(z)}{C_0(z = H_b)}\right)^{0.4} \quad \text{(A39)}$$

c) Bulk gas exchange between emulsion and bubbles to maintain the gas flow in the emulsion phase at minimum fluidization conditions, $u_{mf}$. Note that, the gas suffers from a volumetric expansion during methane conversion in the fuel reactor. So, the excess of the gas in the emulsion, $F_{exc}$, must move to the bubble phase to maintain the minimum fluidization condition in the emulsion.

## 4. Nomenclature

| | |
|---|---|
| $C_b$ | gas concentration in the bubble phase (mol/m$^3$) |
| $C_{db}$ | concentration of solids in the dense bed (kg/m$^3$) |
| $C_{dil}$ | gas concentration in the dilute region (mol/m$^3$) |
| $C_e$ | gas concentration in the emulsion phase (mol/m$^3$) |
| $C_{frb}$ | concentration of solids in the freeboard (kg/m$^3$) |
| $C_p$ | gas concentration in the particle (mol/m$^3$) |
| $C_{ps}$ | gas concentration in the particle surface (mol/m$^3$) |
| $d$ | stoichiometric coefficient for fuel combustion with $O_2$ (mol fuel per mol $O_2$) |
| $d_{react}$ | diameter of the reactor (m) |
| $E_k$ | activation energy of the kinetic constant (J/mol) |
| $F_{exc}$ | excess flow in the emulsion with respect the minimum fluidization (mol/s) |
| $F_i$ | molar flow of gas *i* (mol/s) |
| $g$ | gravity acceleration (=9.8 m s$^{-2}$) |
| $H_b$ | height of the dense bed (m) |
| $H_r$ | height of the reactor (m) |
| $k_{be}$ | mass transfer coefficient between bubble and emulsion phases (s$^{-1}$) |
| $\left(-\overline{r}_{g,i}\right)$ | average gas reaction rate of gas *i* (mol m$^{-3}$ s$^{-1}$) |
| $\left(-\overline{r}'_{g,i}\right)_p$ | average gas reaction rate of gas *i* in the particle (mol m$^{-3}$ s$^{-1}$) |
| $\left(-\overline{r}_{OC,i}\right)$ | average reaction rate of oxygen carrier with gas *i* (mol m$^{-3}$ s$^{-1}$) |
| $t$ | time (s) |
| $u_g$ | gas velocity (m/s) |
| $u_{mf}$ | minimum fluidization gas velocity (m/s) |
| $u_{s,c}$ | velocity of solids in the core (m/s) |
| $u_{tf}$ | velocity of through flow gas (m/s) |
| $u_{vis}$ | velocity of visible bubbles (m/s) |
| $V$ | volume (m$^3$) |
| $y_i$ | molar fraction of gas *i* (-) |
| $z$ | position in the axial direction (m) |

Greek symbols

| | |
|---|---|
| $\delta_b$ | volumetric fraction of bubbles (-) |
| $\varepsilon$ | porosity of the bed (-) |
| $\xi_{g-s}$ | contact efficiency between gas and solids in the dilute region (-) |
| $\rho_{OC}$ | solids density (kg m$^{-3}$) |

## 5. References


Abad A, Gayán P, de Diego LF, García-Labiano F, Adánez J. 2013. Fuel reactor modelling in chemical-looping combustión of coal: 1. Model formulation. Chem. Eng. Sci., 87, 277-293.

Broadhurst, T.E., Becker, H.A., 1975. Onset of fluidization and slugging in beds of uniform particles. AIChE J. 21, 238-247.

Darton, R.C., LaNauze, R.D., Davidson J.F., Harrisson, D., 1977. Bubble growth due to coalescence in fluidized beds. TransIChemE 55.

de Diego, L.F., Gayán, P., Adánez, J., 1995. Modelling of flow structure in circulating fluidized beds. Powder Technology 85, 19-27.

Dewaele, O., Froment, G.F., 1999. TAP Study of the Mechanism and Kinetics of the Adsorption and Combustion of Methane on $Ni/Al_2O_3$ and $NiO/Al_2O_3$. Journal of Catalysis 184, 499-513.

Furusaki, S., Kikuchi, T., Miyauchi, T., 1976. Axial Distribution of Reactivity Inside a Fluid-Bed Contactor. AIChE J. 22, 354-361.

Grace, J.R., 1986. Contacting modes and behaviour classification of gas—solid and other two-phase suspensions. Canadian Journal of Chemical Engineering 64, 353-363.

Pallarès, D., Johnsson, F., 2006. Macroscopic modelling of fluid dynamics in large-scale circulating fluidized beds. Progress in Energy and Combustion Science 32(5-6), 539-569.

Pröll T, Kolbitsch P, Bolhàr-Nordenkampf J, Hofbauer H. 2009. A novel dual circulating fluidized bed system for Chemical Looping processes. AIChE J., 55, 3255-3266.